IRSTI 49.40.37 https://doi.org/10.26577/phst202512114

**D.M. Zhexebay , A.A. Skabylov , D.A. Turlykozhayeva ,**
**A. Bolysbay , U.K. Turmaganbet* , T. Namazbayev ,**
**M. Tao**

School of Electronics and Information, Northwestern Polytechnical University, Xi'an, China
*e-mail: uturmaganbet@gmail.com

# Real-time small object detection with YOLOv8n/8s and YOLOv11n/11s models in complex natural landscapes

Unmanned Aerial Vehicles (UAVs) are increasingly employed for real-time object detection in critical applications such as security surveillance, disaster response, and environmental monitoring. However, accurate detection in UAV imagery remains challenging due to small target sizes, cluttered backgrounds, and varying environmental conditions. This study evaluates the performance of YOLOv8n/v8s and YOLOv11n/11s models for human detection in UAV-captured imagery across diverse natural landscapes. To ensure practical deployment in resource-constrained environments, the models were implemented on a Raspberry Pi 5 using the OpenVINO framework. Experimental results show that both YOLO series achieve comparable detection accuracy in the range of 80–82%, with YOLOv8n and YOLOv11n demonstrating the highest processing speeds of 10.50 and 11.04 frames per second (FPS), respectively. These findings confirm the feasibility of using lightweight YOLO models for real-time human detection on embedded systems. The results highlight the potential of integrating edge AI and UAVs for autonomous, on-site monitoring in remote or complex terrains, offering scalable solutions for intelligent aerial surveillance.

**Key words:** UAV, object detection, accuracy, YOLO models.
**PACS number(s):** 01.30.−y, 07.05.Pj.

## 1 Introduction

Unmanned Aerial Vehicles (UAVs), commonly known as drones, are aircraft that operate without direct human control, relying on remote radio signals or autonomous programming. In recent years, they have been widely adopted in both civilian and military sectors, with applications in agriculture, aerial photography, public safety, ecological protection, and military operations. Their increasing popularity stems from key advantages such as compact size, versatility, and cost-effectiveness [1-3].

Despite these advancements, detecting small objects using UAVs in complex natural environments remains a major challenge. High-altitude perspectives reduce objects to a few pixels, making feature extraction difficult for YOLO models. Scale variations, background clutter, and occlusion further complicate detection, as small objects are often obscured by vegetation, shadows, or other elements. Additionally, dynamic conditions like lighting changes, motion blur, and atmospheric disturbances impact image clarity, further degrading detection performance [3-9].

To solve the above-mentioned problems authors [1] for small object detection proposed UAV-YOLOv8 model with Wise-IoUv3, BiFormer attention, and the Focal FasterNet Block, resulting in high detection accuracy. In [2] authors, optimized YOLOv8 variant achieving good mAP@0.5 while reducing computational complexity. For structured environments, WeiSun et.al introduced the RSOD algorithms[3] an improved YOLOv3-based model for UAV traffic monitoring with VisDrone-Det2018 and UAVDT datasets. To expand object detection beyond the visible spectrum, Jiang et.al. proposed a thermal infrared (TIR) detection framework [4] using YOLO models for FLIR cameras. The YOLOv5s model reached great mAP at 50 FPS, proving effective under low-visibility conditions. Chang et.al. explored enhancements for high-altitude small object detection [5], where SPD-convolution, coordinate attention, transposed convolution, and Alpha-IoU loss were incorporated, improving precision, accuracy, and recall in YOLOv5s. Han et.al. designed, the Senselite model [6] with GSConv, SlimNeck, and a squeeze-and-excitation mechanism, reaching to high mAP@0.5, surpassing YOLOv5 in computational efficiency. For urban road monitoring, Wang et.al. optimized YOLOv9-based model [7], which developed with SCRCONV, SPPELANBRA, and Inner-MP-DIOU loss, achieving state-of-the-art results on the CICVAC dataset. Zhang et.al. introduced, RTS-NET a real-time detection network [8] for UAV patrols, achieving superior mAP and 163.9 FPS, prioritizing real-time efficiency. Zheng et al. analyzed YOLO-based deep learning models [9] across multiple applications, including agriculture, fire detection, ecology, marine science, and UAV navigation. Muzammul et.al. presented, a quantum-inspired multi-scale detection model [10] for ultra-small object detection, incorporating sub-pixel convolution, adversarial training, and self-supervised learning. These above discussed articles exhibited relatively good efficiency in small object detection, however these results can be further improved in terms of speed and accuracy.

In this article, we propose an advanced real-time object detection model for UAV-based surveillance using the latest YOLOv8n/v8s and YOLO 11n/11s, integrated with the OpenVINO framework on Raspberry Pi 5 to optimize speed, accuracy, and efficiency across diverse environments. The latest YOLO versions [11] provide significant advancements in precision, processing speed, and adaptability for various detection tasks, and we believe that the proposed integrated model can further enhance computational efficiency.

The article is structured as follows: Section 2 introduces the YOLO models and their architecture, highlighting key improvements and design choices. Section 3 describes the datasets and processing methods, including data collection, and preprocessing techniques. Section 4 discusses the detection model, detailing training strategies and optimization techniques. Finally, Section 5 presents the results, analyzing model performance in terms of accuracy, efficiency, and real-time applicability in UAV-based object detection.

## 2 Background

### *2.1. YOLO series*

This section presents an overview of the most widely used YOLO object detection models − YOLOv8n/s, YOLOv11n/s − developed in recent years [11,12].

YOLOv8 represents the latest and most advanced iteration in the YOLO series, offering five different models optimized for various scales: YOLOv8n, YOLOv8s, YOLOv8m, YOLOv8l, and YOLOv8x. As depicted in Figure 1, the architecture of YOLOv8 is composed of three core layers: the backbone, the neck, and the detection head [11,12].

The Backbone Layer is built on CSPDarknet53 [12], leveraging five down sampling stages to extract multi-scale features. Unlike previous YOLO versions, YOLOv8 replaces the conventional Cross Stage Partial (CSP) module with the C2f module, which incorporates both dense and residual connections, improving gradient flow and feature representation. Additionally, it integrates the Spatial Pyramid Pooling Fast (SPPF) module, enabling enhanced multi-scale feature extraction while reducing computational complexity and inference latency. This combination ensures a lightweight yet powerful backbone capable of detecting small and large objects efficiently.

The Neck Layer utilizes a fusion of Feature Pyramid Network (FPN) [13,14] and Path Aggregation Networks (PANet) to enhance feature propagation and multi-scale detection. FPN's top-down structure improves the transmission of high-level semantic features to lower layers, aiding small object detection. PANet strengthens feature reuse with a bottom-up pathway, enriching the spatial information flow. Though PANet increases computational cost, its integration with C2f modules balances efficiency and performance, allowing YOLOv8 to capture objects of varying scales with high precision.

The Detection Head Layer adopts a decoupled head structure, separating classification and regression tasks for better optimization. YOLOv8 moves away from traditional anchor-based methods, implementing the Task-Aligned Assigner [15], which dynamically assigns positive and negative samples during training, improving detection accuracy. Classification is handled using binary cross-entropy loss (BCE Loss), while bounding box regression benefits from distribution focal loss (DFL) [16] and Complete Intersection over Union (CIoU) [17] loss. These loss functions refine object localization by penalizing misaligned bounding boxes and improving convergence speed.

One of the features of YOLOv8 is the C2f module, which enhances the gradient flow throughout the backbone and neck. This is achieved by incorporating more skip connections and removing convolutions in its branches, taking inspiration from the C3 module and ELAN design in YOLOv5. Further-more, YOLOv8 introduces a decoupled head that separately processes the extraction of target position and category information, significantly improving detection accuracy. Another important innovation is the shift from conventional anchor-based design to anchor-free architecture. For classification, YOLOv8 utilizes VFL loss, while DFL loss and CIOU loss are employed for regression tasks [18]. To enhance bounding box regression, YOLOv8 employs IoU-based loss functions [19], which evaluate the overlap between predicted and ground truth bounding boxes. While standard IoU Loss struggles in cases of non-overlapping boxes, CIoU mitigates this issue by minimizing the normalized distance between box centers and incorporating an aspect ratio penalty. This leads to faster convergence, superior localization accuracy, and improved performance in detecting small and fast-moving objects [18,19].


**Figure 1** – Structure of YOLOv8 [18]

YOLOv11, the latest version in the YOLO series, brings notable advancements in speed, accuracy, and feature extraction. Like YOLOv8, the architecture of YOLOv11, as depicted in Figure 2, consists of three main components: the backbone, the neck, and the head.

The backbone is the initial and crucial component of YOLOv11, tasked with extracting key features from the input image at various scales. YOLOv11 incorporates C3K2 blocks, which replace the C2f blocks found in YOLOv8 [13]. The C3K2 blocks provide a more computationally efficient implementation of Cross-Stage Partial (CSP) [14]. Additionally, the last two blocks of the backbone are the Spatial Pyramid Pooling Fast (SPPF) and Cross-Stage Partial with Spatial Attention (C2PSA) [16, 19]. The SPPF block uses multiple max-pooling layers to efficiently capture multi-scale features, while the C2PSA block integrates an attention mechanism to improve the model's accuracy.

The neck is the second major component of YOLOv11. As shown in Figure 2, it includes several Conv layers, C3K2 blocks, Concat operations, and Upsample blocks, all enhanced by the C2PSA mechanism. The neck's primary role is to combine features from different scales and forward them to the head for final prediction [20].

The head is the final component of YOLOv11 and plays an essential role in generating predictions. It is responsible for determining the object class, calculating the objectness score, and accurately predicting the bounding boxes for detected objects [21].

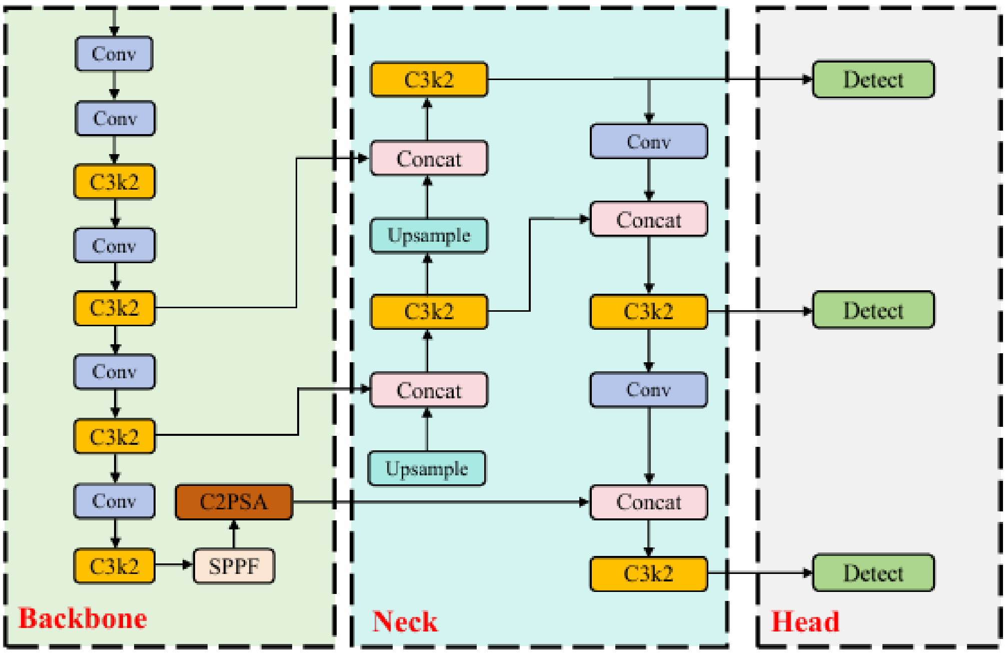


**Figure 2** – Structure of YOLOv11[22]

One of the features of YOLOv11 is the C3PSA module, which provides efficient feature extraction and an advanced attention mechanism for better accuracy. It adopts an anchor-free design and a refined decoupled head for improved localization and classification. Also, optimized loss functions, including VFL and DFL, further enhance precision and stability [22].The model is optimized for modern GPUs [23,24], boosting speed and reducing latency for fast, real-time performance. This makes YOLOv11 perfect for applications like video surveillance and autonomous systems [25,26] that need quick and accurate object detection.

## 3 Dataset and processing

### *3.1. Image database*

In this study, the UAVSOD-10 dataset was utilized, containing aerial imagery captured by UAVs to facilitate small object detection through deep learning techniques. The UAVSOD-10 dataset contains 844 images and 18,234 annotated instances, each labeled with horizontal bounding boxes (HBB) in VOC format [27]. The image widths range from 1,000 to 4,800 pixels, with a resolution of approximately 0.15 meters. Scale differences [28] in objects of the same or different categories are apparent. The width of the smallest object in image instance is 9 pixels, the biggest width is 312 pixels, and the mean width is 74.85 pixels. The images were captured in a mountainous area of the Liuzhi Special Economic Zone, Guizhou Province, China. To enhance the model's generalization ability and account for various natural conditions, the dataset includes images from different types of terrain, such as mountains, forests, and snowfields. This approach enables the model to be trained on data that represents diverse environments, improving its ability to detect people in complex natural landscapes [28].

The model was trained using the Roboflow [29, 30] platform for data annotation. To accelerate learning, the transfer learning technique was applied, enabling pre-trained models to be adapted for the task of detecting people in images captured by drones. Training was conducted on a system with an Intel Core i9 processor [31] and an NVIDIA GeForce RTX 4090 GPU [32], providing the necessary computational power for effective training. The training hyperparameters were as follows: 600 epochs, a batch size of 16, and a learning rate of 0.01. Various data augmentation techniques, such as rotation, scaling, and brightness variation, were employed to improve the model's ability to handle different lighting conditions and object orientations [32].

Object scales were compared by calculating the area ratio of the object bounding box pixels to the total image. As shown in Figure 3, the image scale is enhanced by segmenting it into pixels within a rectangular grid. YOLO models typically process images at varying scales, where the images undergo magnification ranging from zero to 6x [33].

**Figure 3** – Examples of images showing aerial photographs taken with a drone, at zero and 6x magnification

The training set, consisting of 717 images, is composed of diverse locations in the suburbs of China, including mountainous and forested areas, captured at altitudes ranging from 13 to 30 meters. The validation set, made up of 84 images, is carefully selected to represent a wide range of environmental conditions, supporting the model's generalization across different landscapes. The test set, containing 81 images, is used as a benchmark for evaluating the model's performance in real-world scenarios. The dataset is focused on people detection, ensuring precise and reliable identification from dynamic aerial perspectives.

*3.2. Performance of YOLOv8/v11*

The Raspberry Pi 5 is a powerful single-board computer designed for high-performance and real-time processing. It features a 64-bit Broadcom BCM2712 processor (Cortex-A76, up to 2.4 GHz) and a VideoCore VII GPU (800 MHz), offering significant improvements over previous models. With 4 GB or 8 GB LPDDR4X-4267 RAM, it efficiently handles multitasking and large datasets. The PCIe 2.0 interface supports external accelerator integration, enhancing data processing capabilities. Despite a 5A and 5V power requirement, the Raspberry Pi 5 remains compact and efficient for various applications [34-37].

To deploy YOLOv8 and YOLOv11 on Raspberry Pi 5, the trained models were converted into OpenVINO-compatible format. Using OpenVINO's Model Optimizer, the best.pt file was transformed into an Intermediate Representation (IR) model, optimizing it for efficient execution on resource-constrained devices.

OpenVINO (Open Visual Inference and Neural Network Optimization) is an Intel toolkit that optimizes deep learning models for CPUs, GPUs, FPGAs, and VPUs. It converts models from frameworks like TensorFlow and PyTorch into an IR format using the Model Optimizer, and the Inference Engine ensures efficient execution. Integrated with Raspberry Pi 5, OpenVINO enhances inference efficiency, reducing computational overhead and enabling real-time processing using its BCM2712 processor [38] and VideoCore VII GPU [39]. Figure 5 shows the object detection system using Raspberry Pi5.

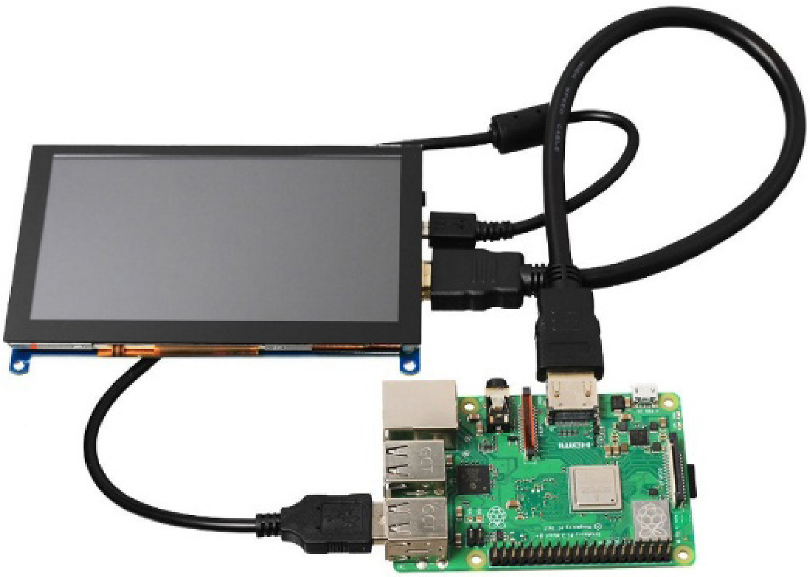

**Figure 5** – Human detection system using Raspberry Pi 5

After the model was converted to the OpenVINO format, the best_yolov8s_openvino_model was deployed on the Raspberry Pi 5. Test images stored in./test/images, and their corresponding YOLO-format annotations in./test/labels were used for evaluation. A Python script on Raspberry Pi 5 handles the entire object detection process : it loads and preprocesses images, performs inference using the YOLO model via OpenVINO, and then compares the predicted bounding boxes with ground truth annotations [40,41]. This comprehensive workflow allows for a detailed assessment of the model's accuracy and performance in real-time object detection on resource-constrained hardware [42].

For each test image, the following steps are performed: the image is loaded into memory, processed through the YOLO model to obtain predicted object coordinates, and compared with ground truth annotations. Bounding boxes are visualized, with predictions in green and actual annotations in red, providing a clear assessment of detection accuracy [43,44]. The inference time for each image is recorded to evaluate real-time performance. Finally, processed images with bounding boxes are saved in the. /results directory for further analysis. This approach ensures a comprehensive evaluation of both detection accuracy and processing efficiency.

## 4 Results

In this section, we evaluate the performance of the YOLO models for addressing the object detection task in real-time applications. Figure 4 presents the detection results of the YOLOv8 and YOLOv11 models in identifying people from UAV imagery under various environmental conditions. In Figure 4, the red bounding boxes represent manually labeled ground truth annotations, while the blue boxes indicate the objects detected by the trained models.

The results shown in Figure 4 indicate that the detection capabilities of the YOLOv8 and YOLOv11 models are acceptable and can be applied in various environmental conditions. The FPS values for each of the tested models are presented in Table 1, enabling a comparison of their processing speeds.

As shown in Table 1, the YOLOv8n and YOLOv11n models achieve the highest FPS (10.50 and 11.04 respectively), indicating their acceptable processing speed and suitability for real-time detection tasks in comparison with other models. Figure 5 presents the results of the confusion matrics and accuracy curves of the YOLOv8n and YOLOv8s models. The x-axis represents the true class labels of the samples, while the y-axis indicates the predicted results.

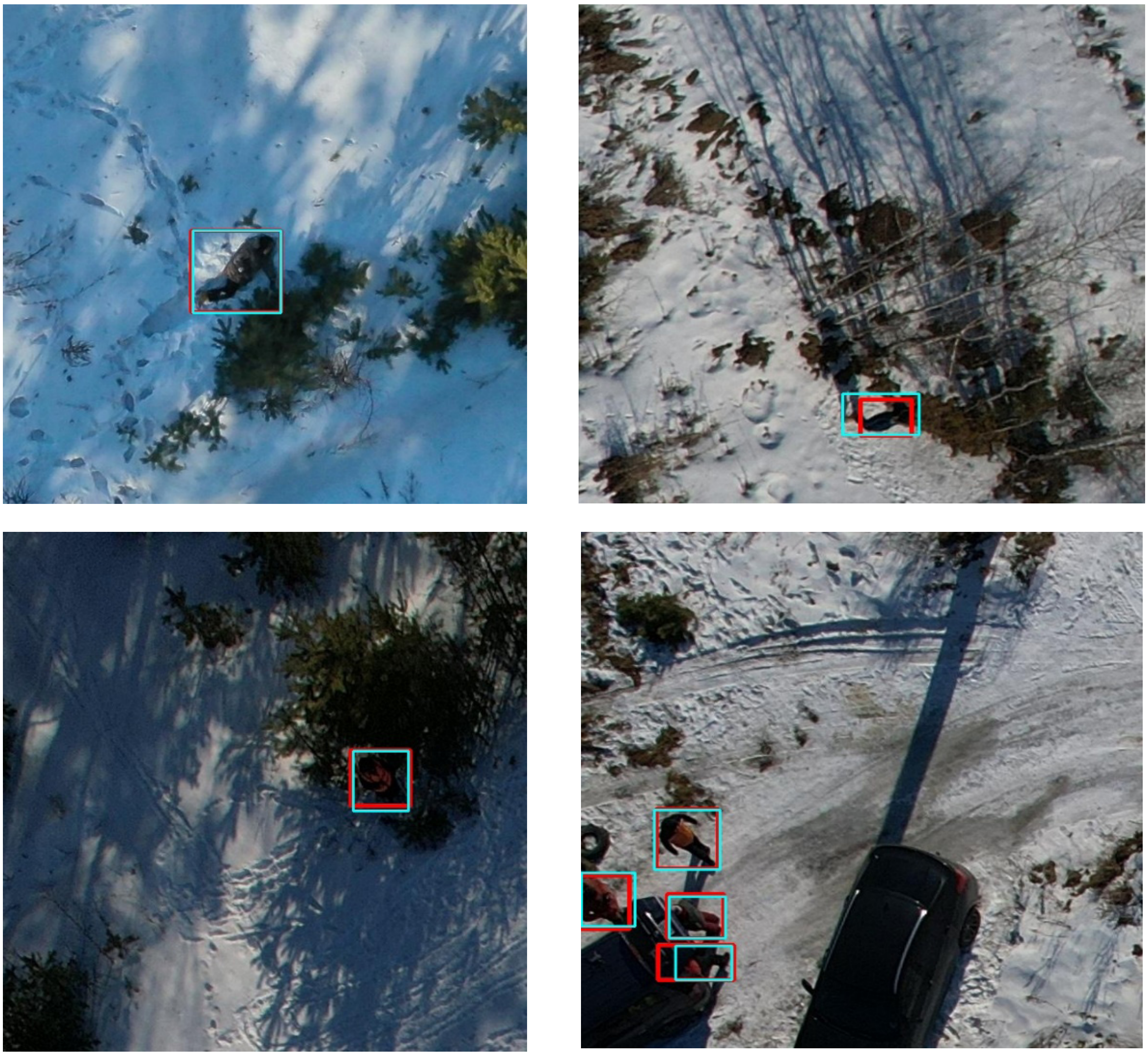

**Figure 4** – Object detection comparison of YOLOv8n/v11n and YOLOv8s/11s models in snow-covered landscapes. Red boxes are ground truth labels, blue boxes are detected objects

**Table 1** – FPS values of the tested YOLOv8 and YOLOv11 models

| Model | FPS |
|---|---|
| YOLO 11s | 5.24 |
| YOLO 11n | 11.04 |
| YOLO v8s | 4.95 |
| YOLO v8n | 10.50 |

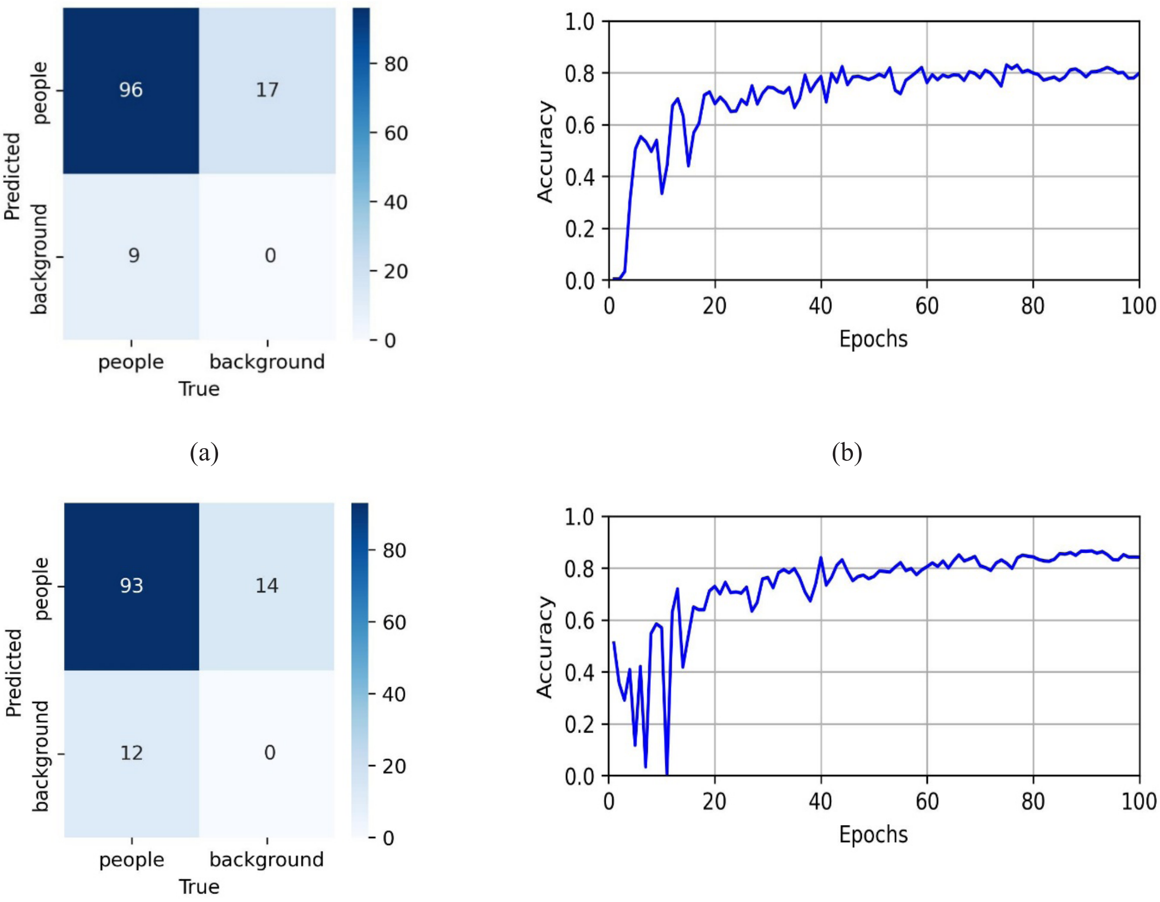


(a) (b)

(c) (d)

**Figure 5** (a, c) – YOLOv8n/s confusion matrix; (b, d) – Accuracy curve

The confusion matrices (a) and (c) show that YOLOv8n detects 96 people, with 17 background and 9 people misclassified, while YOLOv8s identifies 93 people, with 14 background and 12 people misclassified. The accuracy curves (b) and (d) depict the training process over 100 epochs, showing a quick initial improvement before gradually stabilizing around 80%. Figure 6 presents the results of the confusion matrics and accuracy curves of the YOLOv11n and YOLOv11s models.

The confusion matrics (a) and (c) present that YOLOv11n recognizes 94 people and YOLOv11s recognizes 95, with 19 and 22 background instances as people and 11 and 10 people as background, respectively. The accuracy curves (b) and (d) show training progress over 100 epochs, with accuracy stabilizing above 80% after 80 epochs. Figure 7 provides a comparison of the efficiency of YOLOv8n/s and YOLOv11n/s models, showcasing their performance in terms of accuracy and processing speed.

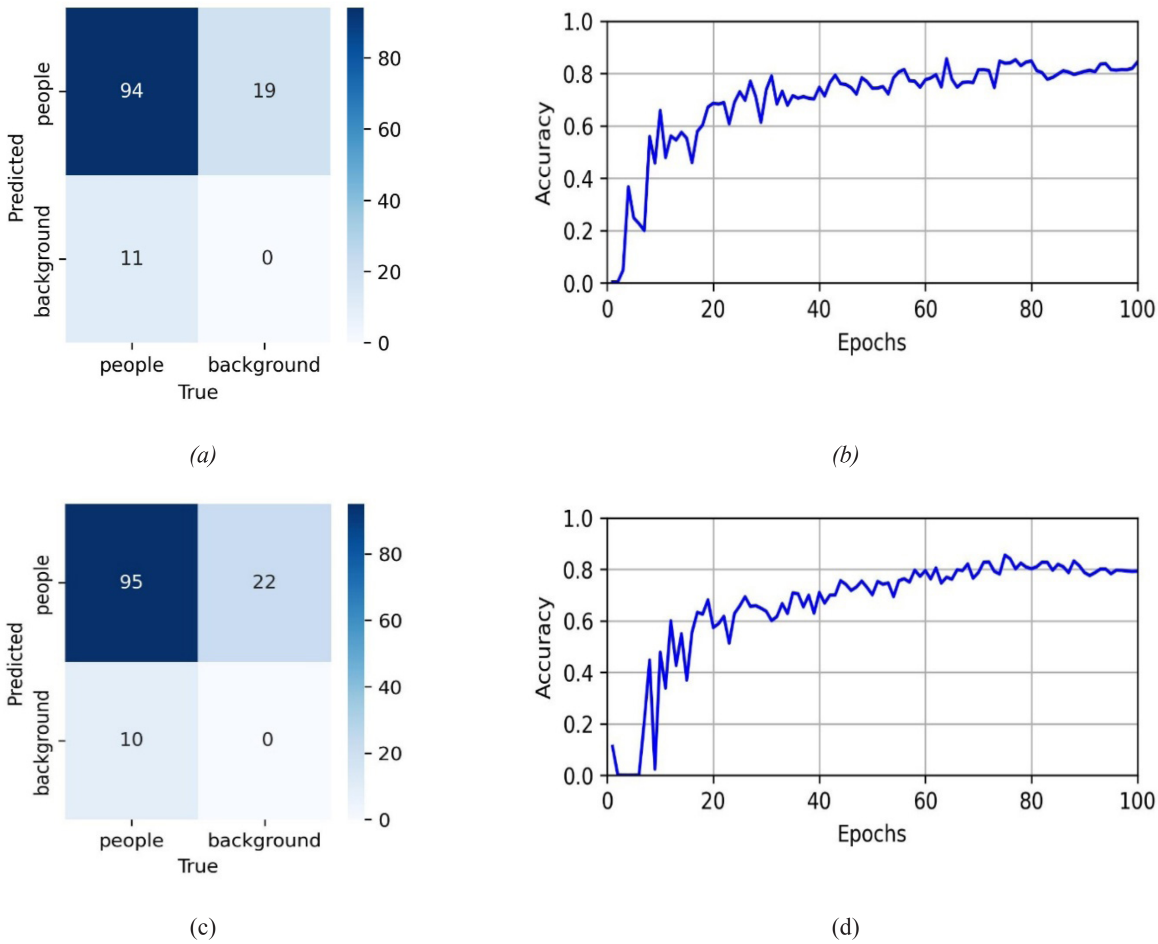


(a) (b)

(c) (d)

**Figure 6** (a, c) – YOLOv11n/s confusion matrix; (b, d) – Accuracy curve

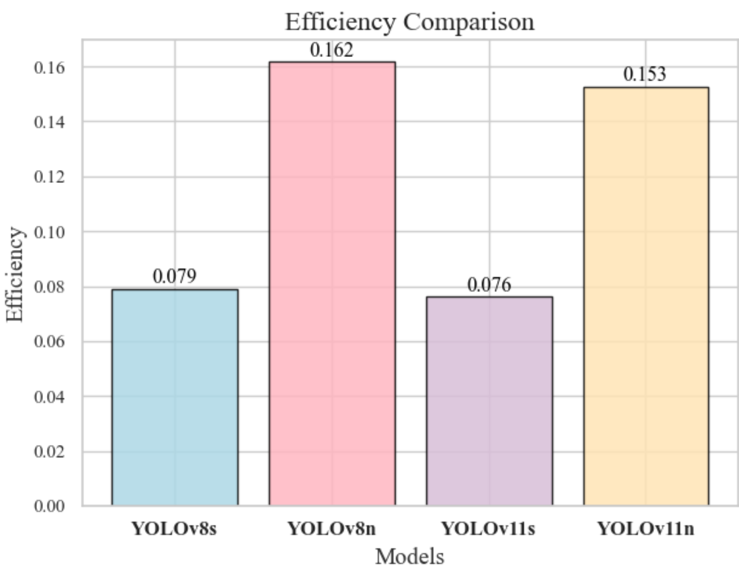


**Figure 7** – Efficiency Comparison of models YOLOv8/11

Figure 7 demonstrates that YOLOv8n and YOLOv11n achieve the highest FPS and accuracy compared to the other evaluated models. Meanwhile, YOLOv8s and YOLOv11s exhibit slightly lower FPS but maintain competitive accuracy, balancing speed and precision in object detection.

## 5 Conclusion

In this article, we have evaluated the performance of YOLOv8n/v8s and YOLOv11n/11s models for human detection in UAV-captured imagery across diverse natural landscapes. The results showed that both YOLO series achieved comparable accuracy between 80% and 82%, with YOLOv8n and YOLOv11n demonstrating the highest FPS. These models exhibited higher efficiency, balancing processing speed and detection accuracy for real-time UAV applications. Their successful deployment on a Raspberry Pi 5 using the OpenVINO framework confirmed their feasibility for real-time object detection in resource-constrained environments.

Future work includes integrating YOLOv8n and YOLOv11n models with FPGA to enhance performance, accuracy, and efficiency for real-time object detection while optimizing computational speed and power consumption for UAV applications.

**Acknowledgments.** We would like to express our sincerest gratitude to the Research Institute of Experimental and Theoretical Physics of the Al-Farabi Kazakh National University for supporting this work by providing computing resources (Department of Physics and Technology). This research was funded by the Ministry of Science and Higher Education of the Republic of Kazakhstan, grant AP19674715 (‘Routing of wireless mesh networks based on box-covering algorithms’).

### References

1. Muzammul M., Assam M., Qahmash A. Quantum-inspired multi-scale object detection in UAV imagery: advancing ultra-small object accuracy and efficiency for real-time applications //IEEE Access. – 2024. – Vol. 10. – P. 2173 – 2186. https://doi.org/10.1109/ACCESS.2024.3523405
2. Wang Y., Zhang J., Zhou J. Urban traffic tiny object detection via attention and multi-scale feature driven in UAV-vision // Scientific Reports. – 2024. – Vol. 14. – Is. 1. – Art. 20614. https://doi.org/10.1038/s41598-024-71074-2
3. Wang J., Yang H., Wu M., Wang S., Cao Y., Hu S., Shao J., Zeng C. UR-YOLO: an urban road small object detection algorithm // Pattern Analysis and Applications. – 2024. – Vol. 27. – Is. 4. – Art. 121. https://doi.org/10.1007/s10044-024-01324-6
4. Han T., Dong Q., Sun L. Senselite: A YOLO -based lightweight model for small object detection in aerial imagery // Sensors. – 2023. – Vol. 23. – Is. 19. – Art. 8118. https://doi.org/10.3390/s23198118
5. Chang Y., Li D., Gao Y., Su Y., Jia X. An improved YOLO model for UAV fuzzy small target image detection // Applied Sciences. – 2023. – Vol. 13. – Is. 9. – Art. 5409. https://doi.org/10.3390/app13095409
6. Sun W., Dai L., Zhang X., Chang P., He X. RSOD: Real-time small object detection algorithm in UAV-based traffic monitoring // Applied Intelligence. – 2022. – Vol. 52. – Is. 4. – P.8448-8463. https://doi.org/10.1007/s10489-021-02893-3
7. Ansah P. A. K., Appati J. K., Owusu E., Boahen E. K., Boakye-Sekyerehene P., Dwumfour A. SB-YOLO-V8: A multilayered deep learning approach for real-time human detection // Engineering Reports. – 2025. – Vol. 7. – Is. 2. – Art. e70033. https://doi.org/10.1002/eng2.70033
8. Vijayakumar A., Vairavasundaram S. Yolo-based object detection models: A review and its applications // Multimedia Tools and Applications. – 2024. – Vol. 83. – No. 35. – P. 83535-83574. https://doi.org/10.1007/s11042-024-18872-y
9. Zeng S., Yang W., Jiao Y., Geng L., Chen X. SCA-YOLO: A new small object detection model for UAV images // The Visual Computer. – 2024. – Vol. 40. – No. 3. – P. 1787–1803. https://doi.org/10.1007/s00371-023-02886-y
10. Jiang C., Ren H., Ye X., Zhu J., Zeng H., Nan Y., Sun M., Ren X., Huo H. Object detection from UAV thermal infrared images and videos using YOLO models // International Journal of Applied Earth Observation and Geoinformation. – 2022. – Vol. 112. – Art. 102912. https://doi.org/10.1016/j.jag.2022.102912
11. Chang Y., Li D., Gao Y., Su Y., Jia X. An improved YOLO model for UAV fuzzy small target image detection // Applied Sciences. – 2023. – Vol. 13. – Is. 9. – Art. 5409. https://doi.org/10.3390/app13095409
12. Wang C. Y., Liao H., Wu Y. H., Chen P. Y., Yeh I. A new backbone that can enhance learning capability of CNN. 2020 IEEE // CVF Conference on Computer Vision and Pattern Recognition Workshops (CVPRW). IEEE. – 2020. – P. 390-391. https://doi.org/10.48550/arXiv.1911.11929
13. Lin T. Y., Dollár P., Girshick R., He K., Hariharan B., Belongie S. Feature pyramid networks for object detection // Proceedings of the IEEE conference on computer vision and pattern recognition. – 2017. – P. 2117-2125. https://doi.org/10.1109/CVPR.2017.106
14. Liu S., Qi L., Qin H., Shi J., Jia J. Path aggregation network for instance segmentation //Proceedings of the IEEE conference on computer vision and pattern recognition. – 2018. – P. 8759-8768. https://doi.org/10.1109/CVPR.2018.00913
15. Feng C., Zhong Y., Gao Y., Scott M. R., Huang W. Tood: Task-aligned one-stage object detection //2021 IEEE/CVF International Conference on Computer Vision (ICCV). – IEEE Computer Society. -2021. – P. 3490-3499. https://doi.org/10.1109/ICCV48922.2021.00349

16. Wang S., Qu Z., Gao L. Multi-spatial pyramid feature and optimizing focal loss function for object detection //IEEE Transactions on Intelligent Vehicles. – 2023. – Vol. 9. – Is. 1. – P. 1054-1065. https://doi.org/10.1109/TIV.2023.3282996

17. Wang X., Song J. ICIoU: Improved loss based on complete intersection over union for bounding box regression // IEEE Access. – 2021. – Vol. 9. – P. 105686-105695. https://doi.org/10.1109/ACCESS.2021.3100414

18. Yue M., Zhang L., Huang J., Zhang H. Lightweight and efficient tiny-object detection based on improved YOLOv8n for UAV aerial images // Drones. – 2024. – Vol. 8. – No. 7. – P. 276. https://doi.org/10.3390/drones8070276

19. Trinh C. D., Do Le T. M., Do T. H., Bui N. M., Nguyen T. H., Ngo Q. U., Bui D. T. Improving YOLOv8 Deep leaning model in rice disease detection by using Wise-IoU loss function // Journal of Measurement, Control, and Automation. – 2025. – Vol. 29. – No. 1. – P. 1-6. https://doi.org/10.3390/agriengineering6010018

20. Wei W., Huang Y., Zheng J., Rao Y., Wei Y., Tan X., OuYang H. YOLOv11-based multi-task learning for enhanced bone fracture detection and classification in X-ray images // Journal of Radiation Research and Applied Sciences. – 2025. – Vol. 18. – Is. 1. – Art. 101309. https://doi.org/10.1016/j.jrras.2025.101309

21. Khanam R., Hussain M. An overview of the key architectural enhancements //arXiv preprint arXiv:2410.17725. – 2024. https://doi.org/10.48550/arXiv.2410.17725

22. He L., Zheng L., Xiong J. FMV-YOLO: A Steel Surface Defect Detection Algorithm for Real-World Scenarios // Electronics. – 2025. – Vol. 14. – No. 6. – P. 1143. https://doi.org/10.3390/electronics14061143

23. Turlykozhayeva D. A., Akhtanov S. N., Zhanabaev Z. Z., Ussipov N. M., Akhmetali A. A routing algorithm for wireless mesh network based on information entropy theory // IET Communications. – 2025. – Vol. 19. – No. 1. –Art. e70011. https://doi.org/10.1049/cmu2.70011

24. Zahoruiko L., Martianova T., Al-Hiari M., Polovenko L., Kovalchuk M., Merinova S., ... Yeraliyeva B. Mathematical model and structure of a neural network for detection of cyber attacks on information and communication systems // Informatics Control Measurement in Economy and Environment Protection. – 2024. – Vol. 14. – No. 3. – P. 49-55. https://doi.org/10.35784/iapgos.6155

25. Kuzminykh V., Koval O., Havrylko Y., Xu B., Yepifanova I., Zhu S., Yeraliyeva B. Synchronization of event-driven management during data collection // Informatyka, Automatyka, Pomiary w Gospodarce i Ochronie Środowiska. – 2024. – Vol. 14. – No. 4. – P. 121-129. https://doi.org/10.35784/iapgos.6656

26. Vasylkivskyi M. V., Horodetska O. S., Savytska L. A., Savina N. B., Kalizhanova A., Komada P. Method to improve information security in fiberoptic systems and networks // Photonics Applications in Astronomy, Communications, Industry, and High Energy Physics Experiments 2024. – SPIE, 2024. – Vol. 13400. – P. 201-207. https://doi.org/10.1117/12.3054856

27. Tymchenko L., Kokriatska N., Pavlov S., Tverdomed V., Lisovenko I., Khomyuk I., Issakozhayeva I. Modified parallel-hierarchical transformation algorithm for processing of optical imaging // Photonics Applications in Astronomy, Communications, Industry, and High Energy Physics Experiments 2024. – SPIE, 2024. – Vol. 13400. – P. 158-163. https://doi.org/10.1117/12.3054898

28. Chen S., Sun Q., Liu M., Tao M., Li Y., Xing M. Superpixel segmentation of marine SAR images based on local fuzzy iteration and edge information for target detection // IEEE Journal of Selected Topics in Applied Earth Observations and Remote Sensing. – 2024. – Vol. 17. – P. 16917-16931. https://doi.org/10.1109/JSTARS.2024.3450548

29. Dong Z., Liu M., Chen S., Tao M., Wei J., Xing M. Occluded SAR target recognition based on center local constraint shadow residual network // IEEE Geoscience and Remote Sensing Letters. – 2025. – Vol. 22. – P. 1-5. https://doi.org/10.1109/LGRS.2025.3532763

30. Liu Y., Tao M., Zhou Y., Zhao L., Su J., Wang L. RFI Localization Scheme for Dual-Channel SAR System based on Alternating Constraints Optimization // 2024 IEEE International Conference on Signal, Information and Data Processing (ICSIDP). – IEEE, 2024. – P. 1-4. https://doi.org/10.1109/ICSIDP62679.2024.10868155

31. Duisebayev T., Ibraimov M., Khaniyev B., Tileu A., Alimbetova D. Development of memory elements based on surface-modified nanostructured porous silicon // WSEAS Transactions on Electronics. – 2024. – Vol. 15. – P. 63-69. https://doi.org/10.37394/232017.2024.15.8

32. Andrushchenko M., Selivanova K., Avrunin O., Palii D., Tymchyk S., Turlykozhayeva D. Hand movement disorders tracking by smartphone based on computer vision methods // Informatyka, Automatyka, Pomiary W Gospodarce I Ochronie Środowiska. – 2024. – Vol. 14. – P. 5-10. http://doi.org/10.35784/iapgos.6126

33. Turlykozhayeva D. A., Akhtanov S. N., Baigaliyeva A. N., Temesheva S. A., Zhexebay D. M., Zaidyn M., Skabylov A. A. Evaluating routing algorithms across different wireless mesh network topologies using NS-3 simulator // Eurasian Physical Technical Journal. – 2024. – Vol. 21, No. 2. – P. 70-82. https://doi.org/10.31489/2024No2/70-82

34. Turlykozhayeva D., Akhtanov S., Zhexebay D., Ussipov N., Baigaliyeva A., Wójcik W., Boranbayeva N. Evaluating machine learning-based routing algorithms on various wireless network topologies // Photonics Applications in Astronomy, Communications, Industry, and High Energy Physics Experiments 2024. – SPIE, 2024. – Vol. 13400. – P. 236-245. https://doi.org/10.1117/12.3058676

35. Ussipov N., Akhtanov S., Zhanabaev Z., Turlykozhayeva D., Karibayev B., Namazbayev T., Tang X. Automatic modulation classification for MIMO system based on the mutual information feature extraction // IEEE Access. – 2024. https://doi.org/10.1109/ACCESS.2024.340044

36. Ussipov N., Akhtanov S., Turlykozhayeva D., Temesheva S., Akhmetali A., Zaidyn M., Tang X. MEGA: Maximum-Entropy Genetic Algorithm for Router Nodes Placement in Wireless Mesh Networks // Sensors. – 2024. – Vol. 24, No. 20. – P. 6735. https://doi.org/10.3390/s24206735

37. Turlykozhayeva D., Temesheva S., Ussipov N., Bolysbay A., Akhmetali A., Akhtanov S., Tang X. Experimental performance comparison of proactive routing protocols in wireless mesh network using raspberry Pi 4 // Telecom. – MDPI, 2024. – Vol. 5, No. 4. – P. 1008-1020. https://doi.org/10.3390/telecom5040051

38. Sabibolda A., Tsyporenko V., Smailov N., Tsyporenko V., Abdykadyrov A. Estimation of the time efficiency of a radio direction finder operating on the basis of a searchless spectral method of dispersion-correlation radio direction finding // IFToMM Asian conference on Mechanism and Machine Science. – Cham: Springer Nature Switzerland, 2024. – P. 62-70. https://doi.org/10.1007/978-3-031-67569-0_8

39. Seidaliyeva U., Ilipbayeva L., Utebayeva D., Smailov N., Matson E. T. LiDAR Technology for UAV Detection: From fundamentals and operational principles to advanced detection and classification techniques // Sensors. – 2024. https://doi.org/10.3390/s25092757

40. Seidaliyeva U., Ilipbayeva L., Taissariyeva K., Smailov N., Matson E. T. Advances and challenges in drone detection and classification techniques: A state-of-the-art review // Sensors. – 2023. – Vol. 24, No. 1. – P. 125. https://doi.org/10.3390/s24010125

41. Temirzhanov A., Sadykov B., Zholdybayev T., Duisebayev B., Ussabayeva G., Kerimkulov Z. STM32F407 microcontroller based multichannel analyzer for spectroscopy // Physical Sciences and Technology. – 2024. – Vol. 11, Nos. 3-4. – P. 21–28. https://doi.org/10.26577/phst2024v11i2b03

42. Solodovnik A. A., Leontyev P. I., Useinov B. M., Kadyrmin A. D., Zyryanov R. O. Application of electronic receivers for recording infrared images of celestial phenomena at the CAR of the NKU // Physical Sciences and Technology. – 2023. – Vol. 10, Nos. 1-2. – P. 50–57. https://doi.org/10.26577/phst.2023.v10.i1.07

43. Saitov E. B., Zikrillayev N. F., Ayupov K. S., Yuldoshev I. A. Determination of the resistance of external parameters to the degradation of the parameters of silicon photocells with input nickel atoms // Physical Sciences and Technology. – 2022. – Vol. 9, Nos. 1-2. – P. 30–36. https://doi.org/10.26577/phst.2022.v9.i1.04

44. Al-Aish A. K. T., Amjed Kamil H. A new system to the spectroscopy analysis with multiple X-ray of free electron laser // Physical Sciences and Technology. – 2024. – Vol. 11, Nos. 3-4. – P. 86–91. https://doi.org/10.26577/phst2024v11i2b010

***Information about authors:***

*Zhexebay Dauren – PhD, Researcher at School of Electronics and Information, Northwestern Polytechnical University (Xi'an, China), e-mail: Dauren.zhexebay@gmail.com*

*Skabylov Alisher – PhD, Researcher at School of Electronics and Information, Northwestern Polytechnical University (Xi'an, China), e-mail: Skabylov.alisher@gmail.com*

*Turlykozhayeva Dana – PhD, Senior researcher at School of Electronics and Information, Northwestern Polytechnical University (Xi'an, China) e-mail: Turlykozhayeva.dana @gmail.com*

*Bolysbay Aslan – BS in Physics, School of Electronics and Information, Northwestern Polytechnical University (Xi'an, China), e-mail: Bolysbay.aslan@kaznu.edu.kz*

*Turmaganbet Ulpan (corresponding author) – MS in Physics, Researcher at School of Electronics and Information, Northwestern Polytechnical University (Xi'an, China), e-mail: uturmaganbet@gmail.com*

*Namazbayev Timu – MS in Physics, Senior researcher at School of Electronics and Information, Northwestern Polytechnical University (Xi'an, China), e-mail: namazbayev.timur@gmail.com*

*Mingliang Tao – PhD, Professor at School of Electronics and Information, Northwestern Polytechnical University (Xi'an, China), e-mail: mltao@nwpu.edu.cn*

*Received April 5, 2025;*
*received in revised form May147, 2025;*
*accepted May 29, 2025*